Int. J. Chem. Sci.: 7(3), 2009, 1987-1999

SURFACE TOPOGRAPHICAL ANALYSIS OF FACE TERMINATED WET THERMAL OXIDATION OF 4H-SiC SUBSTRATE

SANJEEV KUMAR GUPTA*, AMEER AZAM[a] and JAMIL AKHTAR

Sensor and Nanotechnology Group, Semiconductor Devices Area, Central Electronics Engineering Research Institute, PILANI - 333 031 (Raj.) INDIA
[a]Department of Applied Physics, Z. H. College of Engineering and Technology Aligarh Muslim University, ALIGARH - 202002 (U. P.) INDIA

ABSTRACT

The surface topographical analysis of SiO_2 on si-rich and c-rich faces of 4H-SiC has been experimentally analyzed by conductive atomic force microscopy (C-AFM) and surface profiler. Wet thermal oxidation process has been performed in horizontal quartz furnace at 1110ºC with the flow of molecular oxygen from 30 minutes to 180 minutes. Rate of oxidation on c-face has been found nearly 10 times faster than on si-face of 4H-SiC wafer. Stylus based surface profiler and Ellipsometer have been employed for oxidized surface roughness and oxide thickness measurements, respectively. We report that oxidized, c-face contained higher roughness and more atomic density than si-face. The bare surfaces of 4H-SiC faces contribute for the roughness in the respective thermally grown oxides. Si-face surface of 4H-SiC is smoother than c-face surface owing to its epitaxy nature. Atomic scale surface morphology of the oxide on si-face and c-face was captured by employing AFM in constant height mode. A number of samples have been oxidized for each experiment in order to generate statistical data.

Key words : Epitaxial 4H-SiC, Face terminated growth mechanism, Surface roughness, Atomic density

INTRODUCTION

Silicon carbide (SiC) is an emerging, wide band gap semiconductor gaining acceptability for electronic devices particularly for high temperature and harsh environment applications where conventional materials such as silicon and GaAs cease to provide sustainability. There are some 250 polytypes of crystalline SiC, which have been reported in literature[1-7]. The most common polytypes for device application are 4H-SiC,

* Author for correspondence; E-mail: sanjeevgkp@gmail.com;
Tel.: +91-1596252435; Fax : +91-1596242294

6H-SiC, 2H-SiC, 3C-SiC and 15R-SiC where H, C, R refer to hexagonal, cubic and rhombohedral crystal structure, respectively. These all polytypes are different by the repeating layer stacking order, however the hexagonal polytypes 4H (ABCB) and 6H (ABCACB) are the key materials for devices applications, because in addition to their desirable physical and electrical properties wafer up to 3″ in diameter are now commercially available[8]. Among the group of wide band gap semiconductors, SiC competes owing to its unique capability of oxidation in the form of SiO_2 making it an obvious choice for the replacement of mighty silicon. The oxidation growth mechanism of SiC surfaces however has been at its developmental stage. A number of recent publications[8-12] indicate not well understood phenomenon of SiC oxidation. The present work is an experimental addition to the prevailing knowledge of wet thermal oxidation of one of the commercially available device grade polytypes of SiC; 4H-SiC. The faces of hexagonal polytypes of SiC are always terminated into silicon rich and carbon rich faces resulting into si-face and c-face surfaces. The oxidation mechanisms on Si-face and c-face have been found very different however still maintaining SiO_2 composition on both the faces[8]. The magic of the oxidation mechanism on the two faces, therefore, become interesting for exploration[12]. Efforts have been made to understand the oxidation phenomenon by doing dry oxidation[10], ultra thin oxide[13] etc. The polar faces of SiC have different atomic density and roughness. Results of morphological variation in si-face and the c-face dominates the face terminated wet thermal oxidation of 4H-SiC, are presented in this paper.

Thermal oxidation mechanism

The thermal oxidation mechanism of SiC is described by same rules as Si, which is explained by Deal and Grove[14]. During thermal oxidation of silicon carbide, most of the excess carbon is believed to be removed from the interface through the formation of CO_2, which diffuses through the oxide and is thereafter released from the sample surface. However, some of the carbon can remain within the oxide and form carbon clusters or graphitic regions. Such regions near the SiO_2/SiC are expected to be electrically active and could give rise the interface states[15]. The process of SiC thermal oxidation can be divided into three steps. First, the oxidation of the SiC surface occurs through the interaction of an oxygen atom into the chemical bond of a SiC molecule. This oxygen insertion creates a Si-O-C species, which then splits into a CO molecule and a Si atom with a dangling bond. These CO molecules diffuse through the oxide of the oxide surface and react with an oxygen atom, creating CO_2. Second, the Si atom reacts with oxygen atoms, which are at the SiC surface in the initial oxidation or diffuses through the oxide to the oxide SiC interface, forming SiO_2. These three processes can be summarized by the following

reactions

$$SiC + O \longrightarrow CO + Si$$

$$CO + O \longrightarrow CO_2$$

$$Si + 2\,O \longrightarrow SiO_2$$

As opposed to the relatively simple oxidation of Si, there are five steps in the thermal oxidation of SiC.

(i) Transport of molecular oxygen gas to the oxide surface,

(ii) In-diffusion of oxygen through the oxide film,

(iii) Reactions with SiC at the oxide/SiC interface,

(iv) Out-diffusion of product gases (e. g., CO_2) through the oxide film and

(v) Removals of product gases away from the oxide surface.

The last two steps are not involved in the oxidation of Si. The oxidation of SiC is about one order of magnitude slower than that of Si under the same conditions. The first and last steps are rapid and are not rate-controlling steps. But among the remaining steps, the rate-controlling step is still uncertain as discussed in several articles[9]. It has been reported in various research papers that the thermal growth kinetics of SiC is governed by linear parabolic law of Deal and Grove, as derived for Silicon.

$$X_0^2 + AX_0 = B\,(t + \tau) \qquad \ldots(1)$$

In this equation, X denotes oxide thickness where as t is oxidation time. The quantity τ corresponds to a shift in the time coordinate that correct for the presence of the initial layer of oxide thickness and A and B are constants. The above equation is a quadratic equation. The solution of equation can be written as –

$$\frac{X_0}{A/2} = \left(1 + \frac{t + \tau}{A^2/4B}\right)^{1/2} - 1 \qquad \ldots(2)$$

There are two limiting cases of equation (2)

(i) For long oxidation time i. e. thick oxidation equation (2) becomes –

$$X_0^2 = Bt \qquad \ldots(3)$$

This relation is called parabolic law and B is called parabolic rate constant. This limiting case is diffusion controlled case because diffusion flux becomes small as compared to the substrate surface reaction flux. Here, the rate of oxidation is limited by the availability of oxidant at the si–rich interface as well as c–rich interface, which is controlled by the diffusion process.

(ii) For short oxidation time i. e. Thin oxide equation (2) can be written as

$$X_0 = \frac{B}{A}(t+\tau) \qquad \ldots(4)$$

This relation is called linear law and the quantity B/A is called the linear rate constant because in this case, enough oxidant is transported across the oxide layer and the oxidation rate is controlled by concentration of oxidant at the surface[16].

EXPERIMENTAL

Preparation of SiC sample

A 2″ diameter 50 μm epitaxial 4H-SiC wafers of n/n^+ type 8º off-axis oriented were purchased from CREE Research Inc. USA. The wafer has been cut into several pieces using special dicing blade from M/s DISCO Japan. Prior to loading in a horizontal quartz furnace for the oxidation, the wafers were thoroughly cleaned with following chemical cleaning procedure –

Degreasing : There are three incessant steps involved in this cleaning method (a) dip the wafer in 1, 1, 1-trichloroethane (TCE) and boil for 10 minutes (b) dip the wafer in acetone, boil for 10 minutes and then (c) dip the wafer in methanol, boils for 10 minutes followed by rinse the wafer in de-ionized (DI) water[17].

RCA Cleaning : This cleaning method is also known as stranded cleaning (SC). Depending on basic and acidic nature, this method has been divided in two sections. (a) SC-1, solution contains DI water : H_2O_2 : NH_4OH in the ratio of 5 : 1 : 1. Samples were immersed in solution for 10 minutes followed by thoroughly rinse in DI water. To remove the native oxide after this step, samples were dipped in 2% HF for very short time (b) SC-2, solution contains DI water : H_2O_2 : HCl in the ratio of 6 : 1 : 1. Samples were immersed in solution for 10 minutes followed by thoroughly rinse in DI water. 2% HF dip was again repeated to make surface hydrophobic.

Piranha : The solution contains H_2SO_4 : H_2O_2 in the ratio 7 : 1. Samples were

immersed in solution for 10 minutes followed by thoroughly rinse in DI water. Samples were immersed in 2% for very short time to make surface hydrophobic[18]. Finally samples were dried at 150ºC in oven.

Thermal oxidation procedure

Thermal oxidation is accomplished using an oxidation furnace (or diffusion furnace, since oxidation is basically a diffusion process involving oxidant species), which provides the heat needed to elevate the oxidizing ambient temperature. A furnace typically consists of a cabinet, a heating system, a temperature measurement and control system, fused quartz process tubes where the wafers undergo oxidation, a system for moving process gases into and out of the process tubes and, a loading station used for loading (or unloading) wafers into (or from) the process tubes. The heating system usually consists of several heating coils that control the temperature around the furnace tubes. The wafers are placed in quartz glassware known as boats, which are supported by fused silica paddles inside the process tube. A boat can contain many wafers. The oxidizing agent comes with the contact of wafers and diffusion takes place at the interface. In this experiment, wet thermal oxidation is divided in six groups at fixed temperature i. e. 1110ºC for different oxidation time i. e. 30, 60, 90, 120, 150 and 180 minutes. The samples of each group were loaded at 800ºC in the flow of nitrogen for different times as described above, the ramp up and ramp down temperature of furnace 5ºC/min as shown in Fig 1.

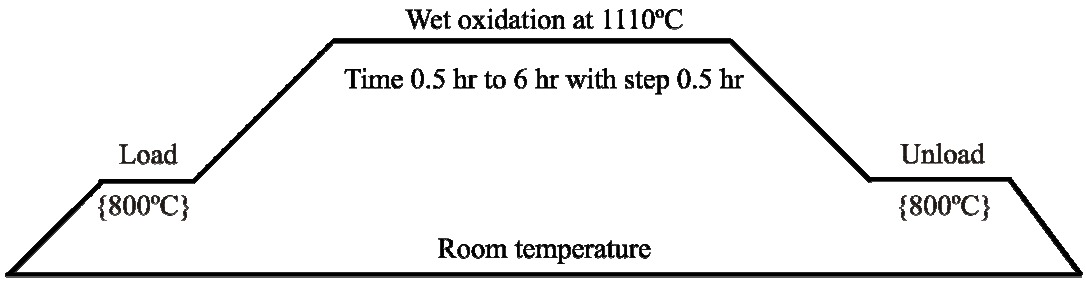

Fig. 1 : Process flow of wet thermal oxidation

RESULTS AND DISCISSION

Roughness analysis

The surface roughnesses on thermally grown oxide as well as bare surface of both terminating faces have been experimentally captured by DAKTEK surface profiler. The profiler have sharply, pointed, conical diamond with a rounded tip stylus, resting lightly on

the surface, is traversed slowly across it and the up and down movement of the stylus relative to a suitable datum are magnified and recorded on a base representing the distance traversed, a graph representing the cross-section will be obtained. Fig. 2 shows the surface texture under the influence of test sample.

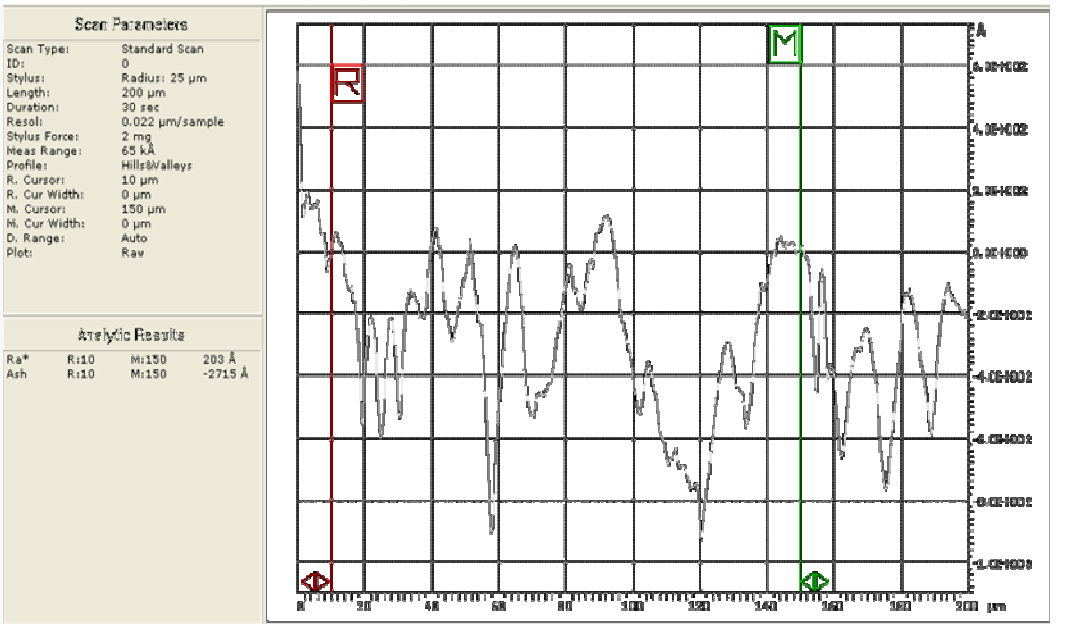

Fig. 2 : Surface roughness measurements employing surface profiler

The above surface texture methodology has been applied to all test samples. At least one sample from all defined group (as described above), treated for a critical oxidation time have been analyzed. It has been observed that the surface roughness on si-face is always less than that of c-face. Fig. 3 and 4 show, the plot regarding to the roughness of thermal oxide covered substrate, which is always greater than bare surface. The surface analysis has been performed by the examination of the correlation between the heights of the surface points through the height to height correlation functions with nearest atom. Oxide roughness on si-face is found 30 to 50 Å where as c-face contain 200 to 250 Å. This roughness of the oxide on c-face as well as si-face is the extended from the bare surfaces of the individual face prior to thermal oxidation. The chemistry of each face influences the oxidation mechanism resulting into vast variations in the oxidation rates on the faces.

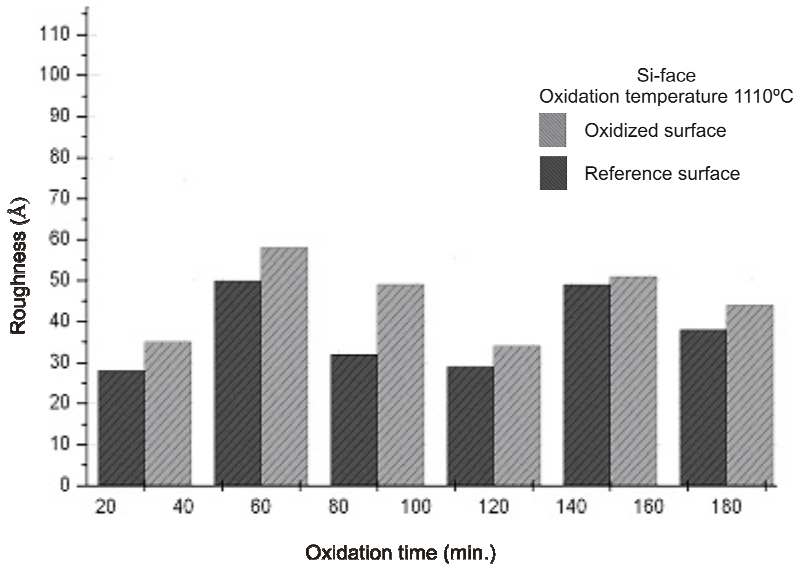

Fig. 3 : Roughness on oxidized si-face compared with bare si-face

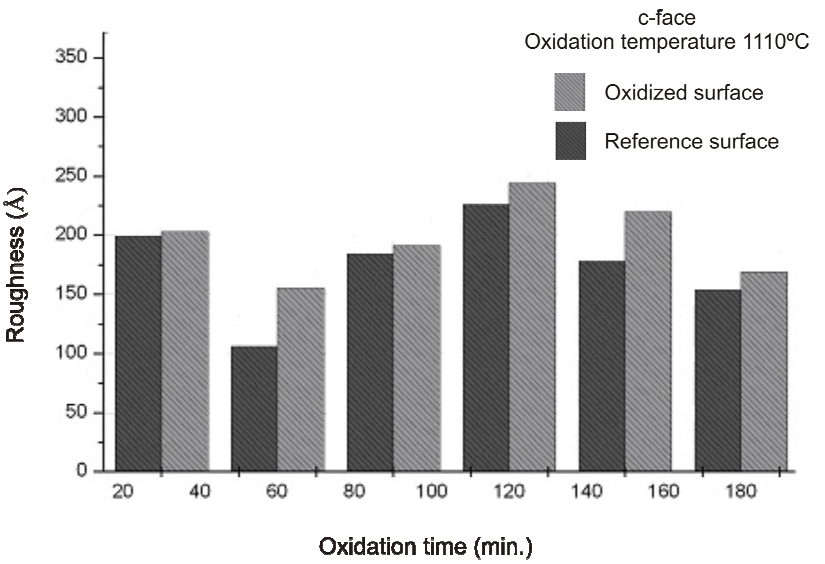

Fig. 4 : Roughness on oxidized c-face compared with bare c-face

Atomic topography analysis

A 4H-SiC sample treated for the oxidation for a time of 60 minutes has been considered in this work. Atomic scale surface morphology of the oxide on c-face and si-face was captured by employing AFM in constant height mode. The sample was imaged, before and after the oxidation, at many different locations on the surface, in order to obtain an average value for the roughness and the other parameters (vertical correlation length, lateral correlation length, roughness exponent). The AFM makes use of a sample-moving scanning device using stacked xy and z stages operating with interferometer and capacitance-based controls of displacements. Image analysis was carried out using nanotech WSxM. Fig. 5(a) shows surface image on si-face where as 5(b) shows on c-face. It has been observed that si-face always predict a smoother topography than c-face.

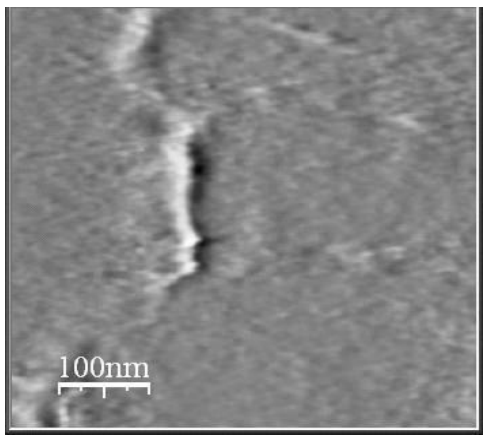

Fig. 5(a) : AFM surface topography on si-face

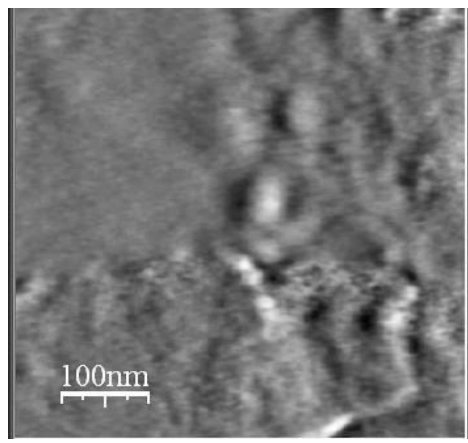

Fig. 5(b) : AFM surface topography on c-face

Besides measuring surface topography, images of other surface physical properties such as atomic arrangement and hardness are measurable with the AFM. In the AFM, it is possible to vibrate the stylus as it is scanned over a surface. Then by measuring the change in phase between the modulating signal and the signal coming from the photo-detector, images of surface hardness are obtained. In this technique, both the surface topography and surface hardness image are acquired simultaneously. Oxide on the c-face shows more atomic density than in case of si-face for same scan area (8 × 8 nm). Fig. 6 (a, b) and 7 (a, b) shows AFM topography on si-face and c-face.

Besides measuring surface topography, images of other surface physical properties such as atomic arrangement and hardness are measurable with the AFM. In the AFM it is possible to vibrate the stylus as it is scanned over a surface. Then by measuring the change in phase between the modulating signal and the signal coming from the photo-detector, images of surface hardness are obtained. In this technique, both the surface topography and surface hardness image are acquired simultaneously. Oxide on the c-face shows more atomic density than in case of si-face for same scan area (8 ×8 nm). Fig. 6 (a, b) and 7 (a, b) shows AFM topography on si-face and c-face.

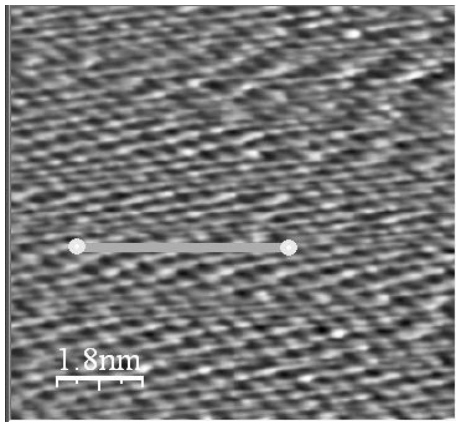

Fig. 6(a) : Atomic nonograph on si-face

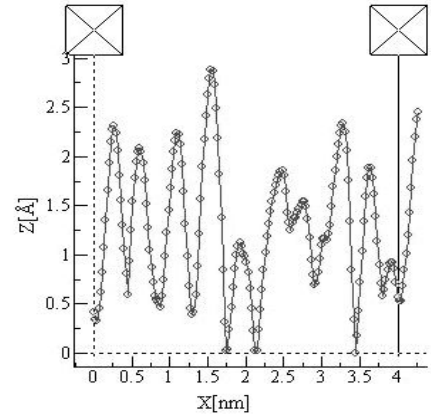

Fig. 6(b) : Line analysis for 4 nm scan length

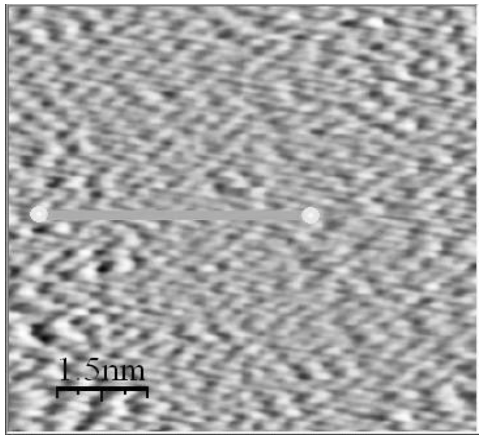

Fig. 7(a) : Atomic nonograph of c-face

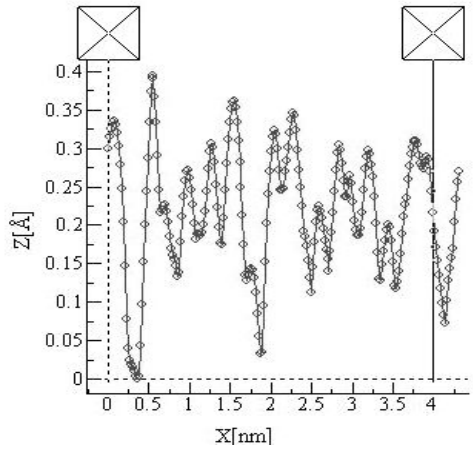

Fig. 7(b) : Line analysis for 4 nm scan length

Thermal oxide growth analysis

Wet thermal oxidation of still the fastest-oxidizing face i. e. the c-face of 4H-SiC is systematically slower than that of Si for identical conditions of temperature, pressure and time. Since the oxidation rate has been shown to depend only feebly on the polytypes for the si-face and not at all for the c-face. It is realistic to believe that although there may be small quantitative differences between the oxidation processes of different polytypes along the perpendicular directions to the bilayer stacking units. The main processes involved in oxidation are diffusion, interface reaction rates and so on, should be largely analogous and so it is practical to discuss oxidations mechanisms without paying special attention to the polytypes. The variable angle spectroscopic Ellipsometer was applied to determine thickness of thermally grown SiO_2 layer on the both terminating faces. The thickness of oxide is verified with measured thickness by DEKTAK surface profiler with realize a sharp step across oxide. Fig. 8 shows a practical measurement of thickness using surface profiler.

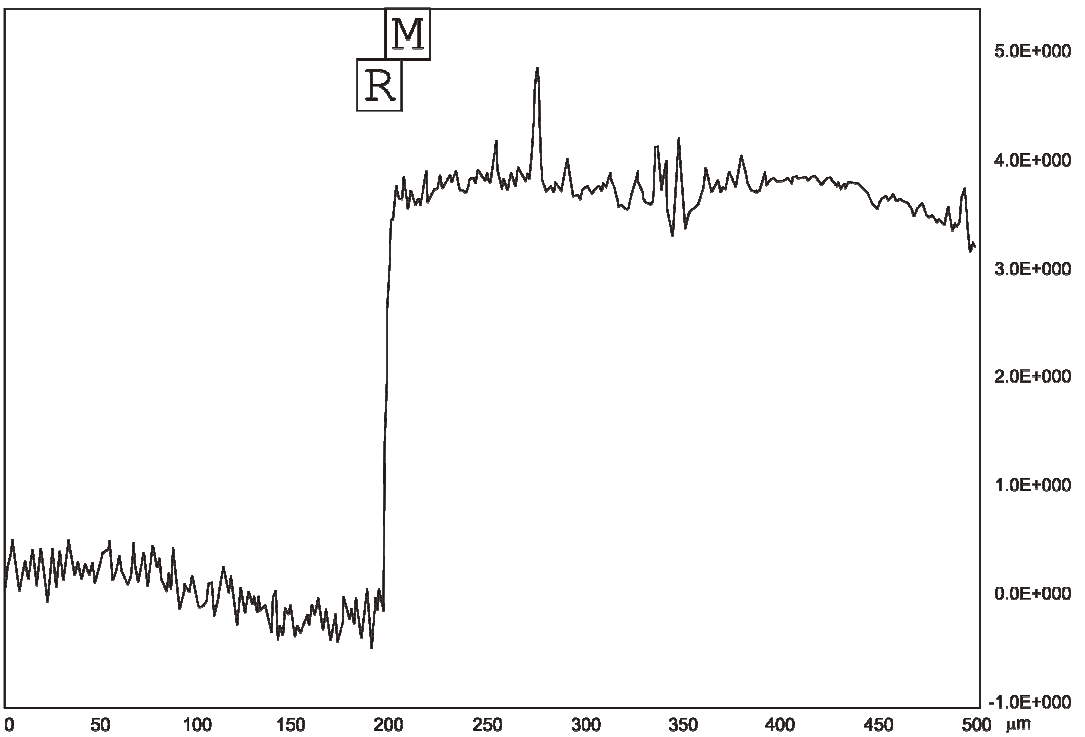

Fig. 8 : Oxide thickness measurements using surface profiler

Each groups associated with four samples, have been thermally treated at critical

temperature as explained above. All obtained values of thickness are plotted as function of oxidation time, which is shown in Fig. 9, explained their face terminated growth kinetics.

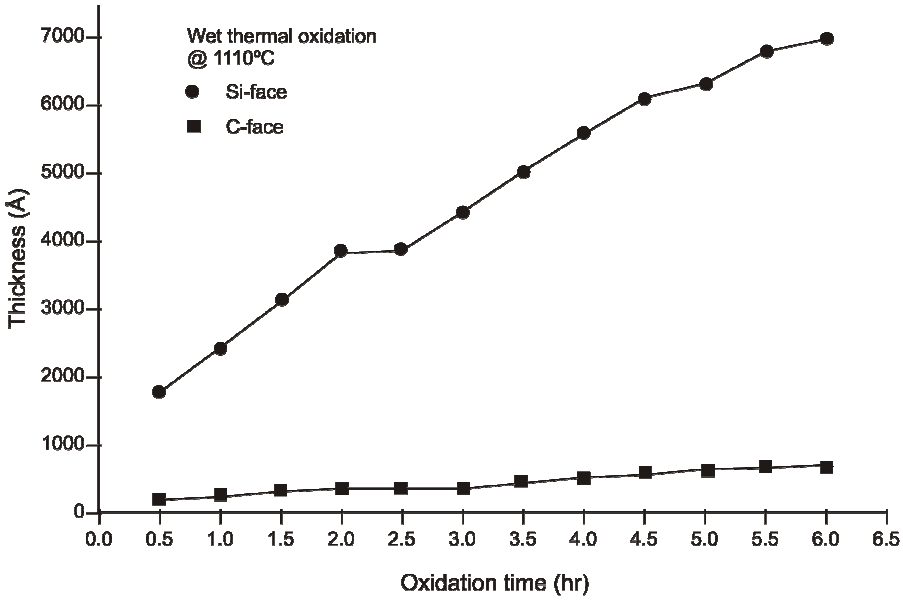

Fig. 9 : Experimental growth of wet thermal oxide on both terminating face

CONCLUSIONS

This article reports a detailed study of the face terminated wet thermally grown SiO_2 and morphological analysis of oxidized as well as bare faces of 4H-SiC substrate. Higher atomic density and more roughness have been found in the case of c-rich face resulted in to fast oxidation rate. This is a process that incorporates the interaction of molecular oxygen with oxidizing species which are present on substrate surface, the different mechanisms through which oxygen is incorporated in the bulk and interface oxide regions during thermal oxidation of 4H-SiC, namely consumption of carbon clusters and reaction with the SiC substrate at both terminating faces. The experimental growth dynamics was quantitatively studied by analyzing statistical plot with different oxidation time.

ACKNOWLEDGEMENT

Authors are grateful to the Director, Dr. Chandra Shekhar, CEERI Pilani, for his kind approval to carry out this work. Support from various teams in the Sensors and

Nanotechnology Group, at CEERI, Pilani, has been the force behind this work. Mr. Gopal Singh Negi, Mr. S. Das, Mr. R. R. Bhatia and Mr. R. N. Soni are gratefully thanked for providing us oxidation facility and necessary help.

REFERENCES

1. S. Nakashima and H. Harima, Phys. Stat. Sol. (a), **162**, 39 (1997).
2. R. P. Devaty and W. J. Choyke, Phys. Stat. Sol. (a), **162**, 5 (1997).
3. J. Q. Liu, H. J. Chung, T. Kuhr, Q. Li and M. Skowronskia, Appl. Phys. Lett., **80**, 2111-2113 (2002).
4. J. P. Bergman, O. Kordina and E. Janzen, Phys. Stat. Sol. (a), **162**, 65 (1997).
5. M. Yu. Gutkin A. G. Sheinerman, T. S. Argunova, J. M. Yi, M. U. Kim, J. H. Jea, S. S. Nagalyuk, E. N. Mokhov, G. Margaritondo and Y. Hwu, J. Appl. Phys., 100, 093518 (2006).
6. W. M. Chen, N. T. Son, E. Janzen, D. M. Hofmann1 and B. K. Meyer1, Phys. Stat. Sol. (a), **162**, 79 (1997).
7. S. A. Reshanova, G. Pensl, H. Nagasawa and A. Schöner, J. Appl. Phys., **99**, 12371 (2006).
8. I. C. Vickridge, J. J. Ganem, G. Battisig and E. Szilagyi, Nuclear Instruments and Methods in Physics Research, **B161-163**, 462- 466 (2000).
9. Y. Song, S. Dhar, L. C. Feldman, G. Chung and J. R. Williams, J. Appl. Phys., **95**, 4953-4957 (2004).
10. J. M. Knaup, P. Deak, T. Frauenheim, A. Gali, Z. Hajnal and W. J. Choyke, Phys., Rev., **B71**, 235321 (2005).
11. K. C. Chang, Y. Cao, L. M. Poter, J. Bentley, S. Dhar, L. C. Feldman and J. R. Williams, J. Appl. Phys., **97**, 104920 (2005).
12. M. Schuermann, S. Dreiner, U. Berges and C. Westphal, Phys. Rev., **B74**, 035309 (2006).
13. P. Fiorenza and V. Raineri, J. Appl. Phys. Lett., **88**, 212112 (2006).
14. B. E. Deal and A. S. Grove, J. Appl. Phys., **36**, 3770 (1965).
15. Eckhard Pippel and Woltersfordf, J. Appl. Phys., **97**, 034302 (2005).

16. E. H. Nicollian and J. R. Brews, MOS (Metal Oxide Semiconductor) Physics and Technology, John Wiley and Sons, New York, (1981) pp. 673.

17. Mariusz Sochacki, Mietek Bakowski and Aleksander Werbowy, Diamond and Related Materials, **11**, 1263-1267 (2002).

18. Mariusz Sochacki, Radoslaw Lukasiewicz, Witold Rzodkiewicz, Aleksander Werbowy and Jan Slzbieta Staryga, Diamond and Related Materials, **14**, 1138 (2005).

Accepted : 21.03.2009